Nonlinearity 3 (1990) 825–850. Printed in the UK

Hopf bifurcation with non-semisimple 1:1 resonance

S A van Gils†, M Krupa‡ and W F Langford§

† Department of Applied Mathematics, University of Twente, PO Box 217, 7500 AE, Enschede, The Netherlands

‡ Institute for Mathematics and its Applications, University of Minnesota, Minneapolis, MN 55455, USA

§ Department of Mathematics and Statistics, University of Guelph, Guelph N1G 2W1, Canada

Received 18 July 1989, in final form 2 April 1990
Accepted by I Stewart

Abstract. A generalised Hopf bifurcation, corresponding to non-semisimple double imaginary eigenvalues (case of 1:1 resonance), is analysed using a normal form approach. This bifurcation has linear codimension-3, and a centre subspace of dimension 4. The four-dimensional normal form is reduced to a three-dimensional system, which is normal to the group orbits of a phase-shift symmetry. There may exist 0, 1 or 2 small-amplitude periodic solutions. Invariant 2-tori of quasiperiodic solutions bifurcate from these periodic solutions. We locate one-dimensional varieties in the parameter space 122^3 on which the system has four different codimension-2 singularities: a Bogdanov–Takens bifurcation, a 132_2 symmetric cusp, a Hopf/Hopf mode interaction without strong resonance, and a steady-state/Hopf mode interaction with eigenvalues $\{0, i, -i\}$. The unfolding of the $\{0, i, -i\}$ singularity gives rise to an invariant 3-torus in the original system. A time-reversal symmetry in the reduced three-dimensional system leads to a degeneracy in the bifurcation of the 3-torus, and Abelian integral calculations imply the possibility of multiple 3-tori in the full equations. We indicate parameter regimes in which the system has the possibility of chaotic dynamics.

AMS classification scheme numbers: 58F14, 34C20

1. Introduction

In the classical Hopf bifurcation theorem for ordinary differential equations, as a pair of complex-conjugate simple eigenvalues crosses the imaginary axis, there is born a unique branch of periodic orbits near an equilibrium point (see Marsden and McCracken [MM76]) or Golubitsky and Schaeffer [GS85], and further references therein). This paper investigates the 1:1 resonant case, in which the purely imaginary eigenvalues at criticality are assumed to be double. Generically, such double eigenvalues are non-semisimple, as assumed here. To date there has been little research on the 1:1 resonant Hopf bifurcation. This bifurcation has been presented as an open problem in Kopell and Howard [KH84] and in Guckenheimer and Holmes [GH83]. A known partial result (due to Caprino *et al* [CMN84] and Vanderbauwhede [Van86]) is that, as a real parameter varies, generically there is either no branch or two branches of periodic solutions depending on the sign of a computable coefficient, in contrast to the unique branch found in the classical Hopf bifurcation; see also Ashkenazi and

0951-7715/90/030825+26$03.50

Chow [AH80], Meyer [Mey84], Atadan and Huseyin [AH85] and Krupa [Kru86]. Some of these authors considered eigenvalues of multiplicity higher than 2, but none determined the stabilities of the bifurcating solutions. We extend these one-parameter results to a three-parameter unfolding of the vector field singularity (which has linear codimension-3), indicate stabilities of the periodic solutions and explore the secondary bifurcations. The relationship of the results obtained here to previous existence results will be discussed in section 3.

Frequently in applications double eigenvalues arise as a result of symmetries, see Golubitsky, Stewart and Schaeffer [GSS88]. In this paper no symmetry is assumed; instead, we have the generic situation in which the double eigenvalues are non-semisimple. This means that they have one-dimensional eigenspaces and two-dimensional generalised eigenspaces (over the complex field). We choose complex coordinates z_1 and z_2 corresponding to the complex eigenvector and generalised eigenvector respectively, and scale these coordinates so that they satisfy

$$0 < |z_2| \ll |z_1| \ll 1. \tag{1.1}$$

This scaling corresponds to solutions which have their principal component in the eigenspace, a choice which is consistent with the previous results on existence of periodic solutions cited above. In other words, our results relate to points (z_1, z_2) contained in a wedge of second order contact around the complex z_1 axis.

The situation in this paper is similar to that in the Hamiltonian Hopf bifurcation. In the class of Hamiltonian systems, if a complex eigenvalue crosses the imaginary axis, then the critical imaginary eigenvalue is forced to be double, and the classical Hopf bifurcation theorem does not apply. As here, the double eigenvalues generically are non-semisimple (and sometimes they are said to be in 1:−1 resonance because the Hamiltonian is indefinite). This case has been studied by Meyer and Schmidt [MS71], Cushman [Cus82] and in more detail by van der Meer [Mee85]. In the present paper the system is not assumed to be Hamiltonian.

Our analysis is based on the Poincaré–Birkhoff normal form for the 1:1 resonant case, which has been computed only recently. It can be expressed as a four-dimensional real system (Cushman and Sanders [CS86]) or as a two-dimensional complex system (Elphick *et al* [ETB87]). Here we use a complex version of the normal form of Cushman and Sanders [CS86]. The nonlinear terms of this normal form vector field commute with a non-compact symmetry group, generated by the transpose of the non-semisimple linearised vector field. One could derive a different normal form, symmetric only with respect to the semisimple part of the linear vector field; see [Bro81], [Bru89].

In the closely related case of non-resonant double Hopf bifurcation with critical eigenvalues $\pm i\omega_1$ and $\pm i\omega_2$, where ω_1 and ω_2 are not rationally related, the truncated normal form has $S^1 \times S^1$ symmetry, and it is possible to reduce the dimension by 2, to a pair of amplitude equations, as in Iooss and Langford [ILa80] or Guckenheimer and Holmes [GH83]. However, in the 1:1 resonant case, the normal form has only one S^1 symmetry, and this permits us to reduce the dimension only by 1, to a three-dimensional system. One consequence of this is that we find richer dynamics than is possible in the two-dimensional amplitude equations of the non-resonant case. Equilibrium points of this three-dimensional system extend to periodic orbits which are relative equilibria of the four-dimensional normal form. The reduction to a three-dimensional system involves a singular change of coordinates, which restricts the applicability of the analysis to the domain (1.1).

In the analysis of this three-dimensional system, we find three different types of codimension-1 singularities and four different types of codimension-2 singularities. The codimension-1 singularities are pitchfork bifurcation, limit point (saddle-node) and Hopf bifurcation. The codimension-2 singularities are a $\mathbb{Z}_2$ symmetric cusp, a Bogdanov–Takens bifurcation, non-resonant double Hopf bifurcation, and a singularity with three critical eigenvalues $\{0, i, -i\}$.

In the $\{0, i, -i\}$ case, we compute the normal form for the system at the singularity, and it turns out to be degenerate: when we set the small parameters equal to zero, the system is time-reversible. As a consequence the terms of order zero in the corresponding amplitude equation vanish identically. We use MAPLE to compute the dependence of normal form coefficients on the small parameters. Having computed the normal form, one obtains a reduction to a particular two-dimensional system which undergoes a Hopf bifurcation as described in [Lan79], [Bro81], [GH83]. This Hopf bifurcation leads one to expect existence of invariant 2-tori in the three-dimensional system, and of 3-tori and intersections of invariant manifolds of 2-tori in the original four-dimensional system. As a consequence of the above-mentioned time-reversibility, the stability coefficient of the Hopf bifurcation in the two dimensional system can pass through 0. This leads to occurrence of degenerate Hopf bifurcations as in [GL81]. We also show that the periodic orbits found in the two-dimensional system can be neutrally stable on a two-dimensional surface in the parameter space. This indicates even richer dynamics for the three-dimensional normal form system and the full four-dimensional system, as in the related cases studied by Chenciner [Che83], Flockerzi [Flo87], and Iooss and Los [ILo89].

The analysis of the 1:1 resonant Hopf bifurcation given in this paper is still not complete. More results could be obtained by extending the analysis developed here; some suggestions for further research are given in the paper. Very often the complexity of the computations stands in the way of obtaining more complete results. Even here the analysis would not have been completed without the help of symbolic computation; the more complicated normal form expressions have been computed with MAPLE. Codimension 1 and 2 bifurcation varieties and some representative bifurcation diagrams have also been computed, using AUTO.

2. Reduction to a three-dimensional system

Let us consider the system

$$\dot{x} = f_\lambda(x) \tag{2.1}$$

where $x \in \mathbb{R}^n$, $\lambda \in \mathbb{R}^3$, $f_\lambda : \mathbb{R}^n \to \mathbb{R}^n$, and $\exists \epsilon > 0$ such that $\forall \lambda$ with $|\lambda| < \epsilon$ we have $f_\lambda(0) = 0$. We assume that $F : \mathbb{R}^{n+3} \to \mathbb{R}^n$, defined by $F(\lambda, x) = f_\lambda(x)$, is C^∞. Suppose that the matrix $A = D_x f_0(0)$ has two equal non-zero imaginary eigenvalues along with their conjugates, $\pm i\omega$, and no other eigenvalues with zero real part. Then, by the centre manifold theorem, the interesting dynamics of (2.1) occurs on a smooth four-dimensional centre manifold, and we may assume without loss of generality that the reduction to this centre manifold has been carried out, so that $n = 4$ in (2.1). With the further assumption that the double eigenvalues are non-semisimple (the generic case), and with a linear change of coordinates and a rescaling of the time t to make

$\omega = 1$, the matrix A can be brought to the form

$$A = \begin{pmatrix} 0 & -1 & 1 & 0 \\ 1 & 0 & 0 & 1 \\ 0 & 0 & 0 & -1 \\ 0 & 0 & 1 & 0 \end{pmatrix}. \tag{2.2}$$

It is often more convenient to work in the complex setting. Let

$$z_1 = x_1 + \mathrm{i}x_2 \qquad z_2 = x_3 + \mathrm{i}x_4 \tag{2.3}$$

and work with $\{z_1, z_2, \bar{z}_1, \bar{z}_2\}$ instead of $\{x_1, x_2, x_3, x_4\}$. After substitution in (2.1), assuming (2.2), we have at $\lambda = 0$

$$\begin{pmatrix} \dot{z}_1 \\ \dot{z}_2 \end{pmatrix} = \begin{pmatrix} \mathrm{i} & 1 \\ 0 & \mathrm{i} \end{pmatrix} \begin{pmatrix} z_1 \\ z_2 \end{pmatrix} + \begin{pmatrix} g_1(z_1, z_2, \bar{z}_1, \bar{z}_2) \\ g_2(z_1, z_2, \bar{z}_1, \bar{z}_2) \end{pmatrix}. \tag{2.4}$$

There is a second pair of equations, for the derivatives of the conjugates $\bar{z}_1$ and $\bar{z}_2$, which we suppress since they are obtained simply by conjugation of (2.4).

Next, we replace equation (2.4) by its *normal form*. The normal form may be computed by a sequence of nonlinear transformations, which eliminate or greatly simplify successively higher order terms in the Taylor expansion of (2.4), up to an arbitrarily high order 'tail' or remainder. Because this procedure does not converge in general, the limit is sometimes called a 'formal normal form'. Convergence is not an issue in the initial analysis, however, since we may stop at any finite order, and by Taylor's theorem we may bound the error in a finite truncation. Then, by standard arguments, we may prove local results, such as for example, that to any hyperbolic periodic solution of the truncated normal form equations there corresponds a nearby periodic solution of the original system. Of course, non-hyperbolic solutions are not necessarily preserved, and smoothness of invariant manifolds may be lost. The general question of what dynamical behaviour is preserved in the normal form, or its finite truncation, remains open at this time.

In fact, in this paper we may avoid the arduous calculation of the normal form coefficients, because our goal is a general classification of the possible solutions. Instead, we employ a formal characterisation by equivariance of the normal form to infinite order, due to Cushman and Sanders [CS86] and Elphick *et al* [ETB87]. Briefly, the above transformation may be carried out in such a way that the only terms remaining in the normal form commute with the elements of the Lie group

$$\mathrm{G} = \{\mathrm{e}^{sA^*} \mid s \in \mathbb{R}\} \tag{2.5}$$

where A^* is the conjugate transpose of A (here taken in the complex form of equation (2.4)). From this fact, it is relatively easy to show that (2.4) has the formal normal form

$$\begin{pmatrix} \dot{z}_1 \\ \dot{z}_2 \end{pmatrix} = \begin{pmatrix} \mathrm{i} & 1 \\ 0 & \mathrm{i} \end{pmatrix} \begin{pmatrix} z_1 \\ z_2 \end{pmatrix} + \phi_1 \begin{pmatrix} z_1 \\ z_2 \end{pmatrix} + \phi_2 \begin{pmatrix} 0 \\ z_1 \end{pmatrix} \tag{2.6}$$

where

$$\phi_k = \phi_k(z_1\bar{z}_1, \mathrm{Im}\,[\bar{z}_1 z_2]) \qquad k = 1, 2. \tag{2.7}$$

Note that the ϕ_ks are G-invariant functions. A real normal form equivalent to (2.6) was first computed by Cushman and Sanders [CS86]. A slightly different representation of this normal form was presented in Elphick *et al* [ETB87].

Let us now consider unfoldings of (2.6). A universal unfolding of the linear vector field $A = \begin{pmatrix} \mathrm{i} & 1 \\ 0 & \mathrm{i} \end{pmatrix}$ is given by

$$A(\lambda) = \begin{pmatrix} \mathrm{i}+\alpha & 1 \\ \mu & \mathrm{i}+\alpha \end{pmatrix} \tag{2.8}$$

where $\lambda = (\alpha, \mu_1, \mu_2)$, $\alpha \in \mathbb{R}$ and $\mu = \mu_1 + \mathrm{i}\mu_2 \in \mathbb{C}$. This is obtained from a four-parameter versal deformation of the corresponding matrix given by Arnold [Arn71], using a time-rescaling to keep the mean imaginary part equal to i. Note that the same result is obtained if we take the constants $\phi_k(0)$ in (2.6) as unfolding parameters for the linear part. The expression for the four eigenvalues is

$$\begin{aligned} &\sigma_k = \mathrm{i} + \alpha \pm \sqrt{\mu} = \mathrm{i} + \alpha \pm (\mu_1^2 + \mu_2^2)^{1/4} \mathrm{e}^{\mathrm{i}(\phi/2 + k\pi)} \qquad k = 1, 2 \\ &\phi \equiv \tan^{-1}(\mu_2/\mu_1) \end{aligned} \tag{2.9}$$

together with the two complex conjugates. Thus we have the natural interpretation of α as a real 'crossing parameter', and μ as a complex 'splitting parameter' for the given eigenvalues $\{\pm i, \pm i\}$. Introducing these parameters into (2.6) and defining $\lambda = (\alpha, \mu_1, \mu_2)$ in (2.1), we arrive at the following G-equivariant parametrised family of formal normal forms

$$\begin{pmatrix} \dot{z}_1 \\ \dot{z}_2 \end{pmatrix} = \begin{pmatrix} \mathrm{i}+\alpha & 1 \\ \mu & \mathrm{i}+\alpha \end{pmatrix} \begin{pmatrix} z_1 \\ z_2 \end{pmatrix} + \phi_1 \begin{pmatrix} z_1 \\ z_2 \end{pmatrix} + \phi_2 \begin{pmatrix} 0 \\ z_1 \end{pmatrix} \tag{2.10}$$

where now

$$\phi_k \equiv \phi_k(\lambda; z_1\bar{z}_1, \mathrm{Im}\,[\bar{z}_1 z_2]) = \mathcal{O}(|z_1|^2 + |z_2|^2) \tag{2.11}$$

uniformly in λ, $k = 1, 2$. In this paper, we study the dynamics associated with the G-symmetric vector field (2.10). We do not claim that (2.10) is a 'universal unfolding' of (2.6), in the sense that *all* the possible dynamics of all the systems neighbouring (2.6) can be obtained by variations of the three parameters (α, μ_1, μ_2), up to some equivalence relation (as is true for the linear case). However, we are able to determine the possible steady-state and periodic solutions (locally), and we can indicate where certain 2-tori, 3-tori and chaotic dynamics may be found.

We make two observations concerning (2.10). First, note in (2.10) that $z_1 = 0$ implies $z_2 = 0$, which is consistent with the ordering (1.1). This suggests that we seek solutions for which z_1 is a factor of z_2, that is,

$$z_2 = z_1 w \equiv z_1(u + \mathrm{i}v) \tag{2.12}$$

where $w = u + \mathrm{i}v$ is a new coordinate. The transformation of coordinates $(z_1, z_2) \to (z_1, w)$ is singular at the origin.

The second observation is that, in addition to the G-equivariance, the normal form has a simpler S^1-equivariance, with respect to the semisimple part of A [Bru89]. Write

$$A = S + N = \begin{pmatrix} \mathrm{i} & 0 \\ 0 & \mathrm{i} \end{pmatrix} + \begin{pmatrix} 0 & 1 \\ 0 & 0 \end{pmatrix} \tag{2.13}$$

and define the Lie group

$$S^1 = \{e^{sS^*} = e^{-is}I \mid s \in \mathbb{R}\}. \tag{2.14}$$

Then it is easily verified that the normal form (2.10) commutes with S^1. Therefore, given any solution $z = (z_1, z_2)$ of (2.10), we obtain a group orbit $S^1 z = \{(e^{-is}z_1, e^{-is}z_2)\}$ of solutions, all with the 'same' dynamics (i.e. S^1-conjugate). We are mainly interested in the dynamics normal to these group orbits; hence we choose new coordinates tangent and transverse to these group orbits. Introduce coordinates (r, θ) satisfying $r > 0$ and

$$z_1 = re^{i\theta} \qquad z_2 = re^{i\theta}w. \tag{2.15}$$

It is clear that the invariant functions ϕ_k in (2.10) are even functions in r, and that the formal normal form is odd in r, i.e. has $\mathbb{Z}_2$ symmetry. Therefore we can make a further reduction, defining

$$\rho = r^2 \qquad (\rho > 0) \tag{2.16}$$

and we have arrived at our final choice of coordinates: (ρ, u, v), normal to the S^1 group orbits, and the phase variable θ, tangent to the group orbits. The normal form (2.10) must now be reexpressed in terms of these new coordinates. The result of this substitution is a set of three real equations, *independent of the phase variable* θ

$$\begin{aligned} \dot{\rho} &= 2\rho[\alpha + u + F_1(\lambda; \rho, \rho v)] \\ \dot{u} &= \mu_1 - u^2 + v^2 + F_3(\lambda; \rho, \rho v) \\ \dot{v} &= \mu_2 - 2uv + F_4(\lambda; \rho, \rho v) \end{aligned} \tag{2.17}$$

together with the phase equation

$$\dot{\theta} = 1 + v + F_2(\lambda; \rho, \rho v) \tag{2.18}$$

where

$$\begin{aligned} \phi_1 &\equiv F_1 + iF_2 \\ \phi_2 &\equiv F_3 + iF_4. \end{aligned} \tag{2.19}$$

We note again that the unfolding parameters in (2.17) can be considered to be the values of $F_k(0)$, and similarly for (2.18).

Together, equations (2.17), (2.18) determine the full four-dimensional dynamics of the formal normal form (2.10), for $\rho > 0$. In general, for a dynamical system with symmetry group G, a point x_0 in the phase space is called a *relative equilibrium* of G if the dynamic orbit $\{x_0(t)\}$ through x_0 lies in the group orbit Gx_0; see [Kru90]. In the present case, it is clear that any equilibrium point with $\rho > 0$ of the three-dimensional system (2.17) yields a relative equilibrium of the four-dimensional system (2.17), (2.18); and of the formal normal form (2.10). Since locally $\dot{\theta} \approx 1$ in (2.18), these relative equilibria are periodic orbits of (2.10). The three-dimensional system (2.17) is the main object of study in the remainder of this paper.

3. Existence of periodic orbits

In this section we find equilibrium solutions of (2.17), corresponding to periodic solutions of (2.10), for small values of both $|w|$ and $\rho > 0$. The principal contribution of the F_k in (2.17) and (2.18) will be from the terms with Taylor coefficients

$$\begin{aligned} a &= \partial_\rho F_3 \qquad & b &= \partial_\rho F_4 \\ d_1 &= \partial_\rho F_1 \qquad & d_2 &= \partial_\rho F_2 \\ d_3 &= \partial_{\rho v} F_3 \qquad & d_4 &= \partial_{\rho v} F_4 \end{aligned} \tag{3.1}$$

evaluated at $(\lambda; \rho, u, v) = (0; 0, 0, 0)$ In the following analysis we assume $a \neq 0 \neq b$.

First we rescale the variables in (2.17) to make the ordering (1.1) explicit, with

$$z_1 = \mathcal{O}(\epsilon) \qquad z_2 = \mathcal{O}(\epsilon^2) \qquad \epsilon \to 0 \tag{3.2}$$

where ϵ is a small scaling parameter to be made precise later. This will 'blow up' the dominant terms in (2.17). We define the rescaled variables by

$$\rho = \epsilon^2 \hat{\rho},\ u = \epsilon \hat{u},\ v = \epsilon \hat{v},\ \epsilon t = \hat{t},\ \alpha = \epsilon \beta,\ \mu_1 = \epsilon^2 \nu_1,\ \mu_2 = \epsilon^2 \nu_2. \tag{3.3}$$

Remark. The parameter α is scaled to a different order in ϵ from the scaling of μ_1 and μ_2 in (3.3). This is necessary to prevent α from disappearing from the rescaled problem as $\epsilon \to 0$. Another reason for such scaling is given by the form of the eigenvalues (2.9), from which it is clear that both the real part $\alpha \pm (\mu_1^2 + \mu_2^2)^{1/4} \cos(\phi/2)$ and the detuning parameter $\pm(\mu_1^2 + \mu_2^2)^{1/4} \sin(\phi/2)$ are rescaled to $\mathcal{O}(\epsilon)$ by (3.3).

After substituting (3.3) and (3.1) into (2.17) and dropping the hats, we have

$$\begin{aligned} \dot{\rho} &= 2\rho(\beta + u + \epsilon d_1 \rho + \mathcal{O}(\epsilon^2)) \\ \dot{u} &= \nu_1 - u^2 + v^2 + a\rho + \epsilon d_3 \rho v + \mathcal{O}(\epsilon^2) \\ \dot{v} &= \nu_2 - 2uv + b\rho + \epsilon d_4 \rho v + \mathcal{O}(\epsilon^2)\ . \end{aligned} \tag{3.4}$$

It is clear from these equations that we can rescale a to ± 1 (having assumed $a \neq 0$), by rescaling ρ with a positive factor. Furthermore, when $\epsilon = 0$, we can assume $b > 0$; since otherwise we could reverse the signs of b, ν_2, v. Hyperbolic solutions with $b < 0$ obtained this way at $\epsilon = 0$ will persist locally for $\epsilon \neq 0$, by standard arguments. So without loss of generality we assume $a = \pm 1$, and $b > 0$.

We proceed to find equilibrium solutions of (3.4). Initially we let $\epsilon \to 0$ in (3.4), and obtain

$$\begin{aligned} \dot{\rho} &= 2\rho(\beta + u) \\ \dot{u} &= \nu_1 - u^2 + v^2 + a\rho \\ \dot{v} &= \nu_2 - 2uv + b\rho. \end{aligned} \tag{3.5}$$

The equilibria of (3.5) with $\rho > 0$ are the roots of the quadratic equations

$$\begin{aligned} 0 &= \beta + u \\ 0 &= \nu_1 + a\rho - u^2 + v^2 \\ 0 &= \nu_2 + b\rho - 2uv\ . \end{aligned} \tag{3.6}$$

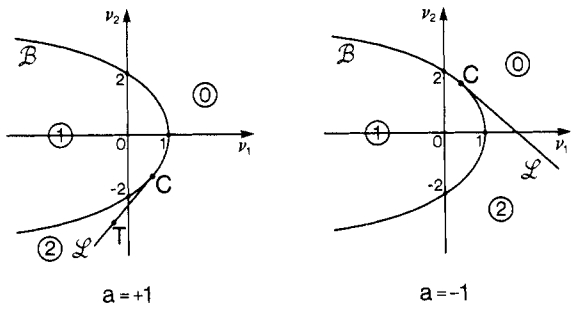

Figure 1. Multiplicities of periodic solutions for $\beta \neq 0$.

Equations (3.6) have the solutions

$$\begin{aligned} u &= -\beta \\ v &= \frac{a\beta \pm \sqrt{D}}{b} \\ \rho &= -\frac{\nu_2 + 2\beta v}{b} \end{aligned} \tag{3.7}$$

where

$$D \equiv b(a\nu_2 - b\nu_1) + \beta^2(1 + b^2). \tag{3.8}$$

The solutions (3.7) are admissible only if v is real and $\rho > 0$. The reality condition is clearly

$$D \geq 0 \tag{3.9}$$

and the condition that ρ be positive is examined more carefully below. By the implicit function theorem, the solutions (3.7) extend smoothly to equilibrium solutions of (3.4) for small $\epsilon > 0$, provided the relevant Jacobian is non-singular. This Jacobian matrix, evaluated at the solution (3.7) with $\epsilon = 0$, is given by

$$J_0 = \begin{pmatrix} 0 & 2\rho & 0 \\ a & 2\beta & 2v \\ b & -2v & 2\beta \end{pmatrix}. \tag{3.10}$$

The determinant and trace of J_0 are

$$\det J_0 = \pm 4\rho\sqrt{D} \qquad \operatorname{tr} J_0 = 4\beta. \tag{3.11}$$

Since we have already required $\rho > 0$ and $D \geq 0$, all the solutions (3.7), except possibly on $D = 0$, are guaranteed to extend locally in ϵ, to equilibria of (3.4), by the implicit function theorem. We have the following theorem.

Theorem 1. For every value of the parameters α, μ_1, μ_2 in a neighbourhood of 0, the equation (2.10) has 0, 1 or 2 periodic orbits which lie inside a wedge of second-order contact about the z_1 plane in the (z_1, z_2) coordinates. For each fixed small $\alpha \neq 0$, the corresponding (ν_1, ν_2) plane has three open connected components, as in figure 1, labeled by the number of periodic orbits in each component. If $\alpha = 0$ then there are two open connected components, containing 0 or 2 periodic solutions, as in figure 2.

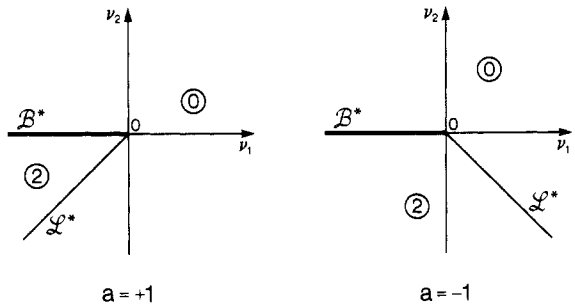

Figure 2. Multiplicities of periodic solutions for $\beta = 0$.

The proof of theorem 1 will follow from the implicit function theorem, hyperbolicity, and standard persistence arguments presented in the next section, after the following two technical lemmas which demonstrate that the roots of the quadratic equations (3.6) have the properties described in theorem 1.

The condition that ρ be positive is more transparent if we first eliminate u and v from (3.6) and obtain the single equation

$$f(\rho) \equiv 1 - \frac{\nu_1 + a\rho}{\beta^2} - \left(\frac{\nu_2 + b\rho}{2\beta^2}\right)^2 = 0 \tag{3.12}$$

provided that $\beta \neq 0$. Under this assumption, we can fix the scaling parameter $\epsilon > 0$ in (3.3) to make $\beta = \pm 1$, with $\epsilon = |\alpha|$.

Lemma 1. Assume $\beta \neq 0$. For given ν_1, ν_2, equation (3.6) has 0, 1, or 2 real roots (ρ, u, v) with ρ positive, as follows.

Case A. Suppose the point (ν_1, ν_2) lies strictly inside the parabola in figure 1, i.e. $f(0) = 1 - \nu_1 - (\nu_2/2)^2 > 0$. Then there is a unique root with ρ positive. This root has Jacobian $J_0 \neq 0$.

Case B. Suppose (ν_1, ν_2) lies outside the parabola, i.e. $f(0) = 1 - \nu_1 - (\nu_2/2)^2 < 0$. Then there are two regions with 0 or 2 real roots $\rho > 0$ respectively, as indicated in figure 1. For each root, $J_0 \neq 0$.

Case C. Suppose (ν_1, ν_2) lies on the parabola, i.e. $f(0) = 1 - \nu_1 - (\nu_2/2)^2 = 0$. Then there are 0 or 1 real roots $\rho > 0$ respectively, depending on whether $b\nu_2 + 2a\beta^2 \geq 0$ or < 0.

Proof. In case A, $f(0) > 0$. Note that f is a quadratic function. Hence its graph will be as in either (*a*) or (*b*) of figure 3, and it is clear that f has two real roots, precisely one of which is positive.

For case B, we note that the discriminant of f is precisely D of (3.8), and the line $D = 0$ is tangent to the parabola in figure 1 at the cusp point $\mathscr{C}$, where $f(0) = \dot{f}(0) = 0$, with coordinates

$$\begin{aligned} \nu_1 &= \beta^2\left(1 - \frac{1}{b^2}\right) \\ \nu_2 &= -\beta^2 \frac{2a}{b}. \end{aligned} \tag{3.13}$$

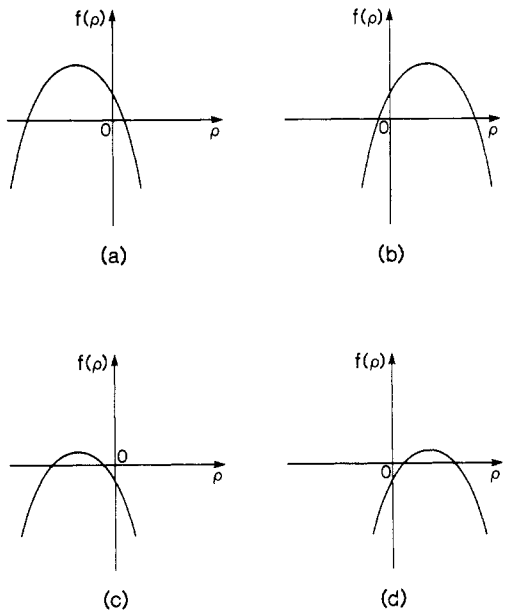

Figure 3. Graph of $f(\rho)$.

The discriminant D is negative on the side of $D = 0$ away from the parabola, so there are 0 real roots in this half-plane. In the remaining cusp regions, $D > 0$ and $f(0) < 0$ imply that the graph of $f(\rho)$ is as in (*c*) or (*d*) of figure 3. An easy calculation shows that the two roots are both positive only for (v_1, v_2) in the cusp with $bv_2 + 2a\beta^2 < 0$, (or $v_2 < -2a/b$ after scaling), as shown in figure 1.

Case C follows similarly.

The codimension-2 point where the parabola touches the line $D = 0$ is the $\mathbb{Z}_2$ symmetric cusp bifurcation (with vanishing cubic bifurcation coefficient), which is discussed in more detail in the next section.

We now describe the degenerate case with $\beta = 0$ for which lemma 1 fails. When $\beta = 0$, obviously we cannot define the scaling parameter ϵ to make $\beta = \pm 1$, as in figure 1. (We may instead choose the scaling such that $v_1 = \pm 1$ in figure 2; however, we defer fixing v_1 for now).

Lemma 2. Assume that $\beta = 0$. Then, except on the ray $\{(v_1, v_2) \mid D = 0, bv_2 < 0\}$, the quadratic equations (3.6) have either 0 or 2 equilibrium solutions with ρ positive. The two solutions exist only in the cone

$$b(av_2 - bv_1) > 0 \qquad \text{and} \qquad bv_2 < 0 \tag{3.14}$$

as shown in figure 2.

Proof. Lemma 2 follows directly from the form of (3.7) with $\beta = 0$.

The connection between figures 1 and 2 becomes more clear if we plot the 3-parameter surface defined by $f(0) = 0$ in equation (3.12), see figure 4. (Figure 4 shows only half of the surface, for $\beta \leq 0$; the half for $\beta \geq 0$ is symmetric.) Level curves of

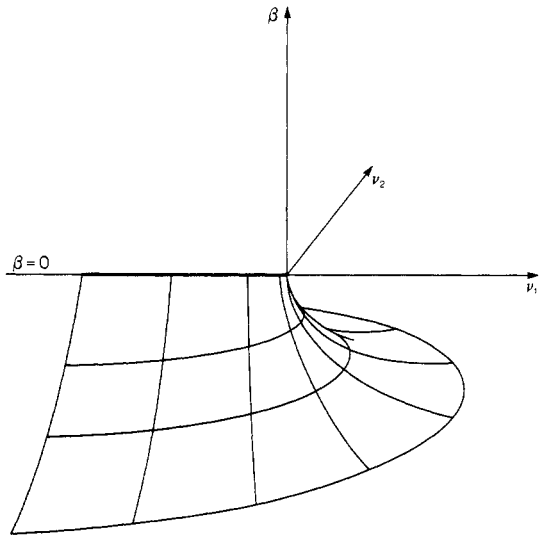

Figure 4. Primary bifurcation surface for $\beta \leq 0$.

the surface in figure 4 are the parabolas in figure 1. As $\beta \to 0$, the surface becomes vertical, and the parabolas degenerate into the ray along the negative ν_1-axis, seen in figure 2.

We end this section with a few remarks on the 'distinguished parameter' approach to this bifurcation problem. The idea is that experimentally one usually varies only one parameter at a time, and it is often enlightening to plot *bifurcation diagrams* which graph the solution branches as this distinguished parameter varies. However if the singularity has codimension greater than one, as here, then there can be many different bifurcation diagrams corresponding to different paths through the singularity. For further discussion of the general situation, see [GS85]. In the present problem we can easily recover the distinguished parameter results as foilows. Normally one assumes that the path is smooth, and can be taken locally in parameter space to be a straight line (non-degeneracy assumption). Therefore we consider a general straight line through the origin in (α, μ_1, μ_2)-space. For a fixed small value of $\epsilon > 0$, this corresponds to a line through the origin in (β, ν_1, ν_2) space, see figure 4. Recall that this surface forms a cusp with vertical tangent along the ray $\beta = 0$, $\nu_2 = 0$, $\nu_1 < 0$. Therefore, a line through the origin locally enters a region 'interior' to the surface only if it lies in a vertical plane ($\nu_2 = 0$) in figure 4. In other words, a generic path through the origin encounters (locally) only regions with 0 or 2 solutions, according to lemmas 1 and 2. This conclusion is in accord with the one-parameter results [CMN84], [Van86], cited in the introduction.

However, one-parameter results still leave much to be desired. One should consider also 'imperfect bifurcation', that is, allow unfolding parameters which displace the path from passing through the singularity, rather than just changing the direction as it passes through. Some of these paths would include bifurcations of single periodic solutions from $\rho = 0$, as in case A of lemma 1, instead of only pairs as in case B. A few examples of such bifurcation diagrams are presented in the numerical results of section 5, where either ν_1 or ν_2 has been chosen as the distinguished bifurcation parameter, and β has been assigned fixed values. Completely different bifurcation diagrams result from other

choices of distinguished parameter. A complete analysis of such bifurcation diagrams, at least insofar as periodic solutions are concerned, is possible using singularity theory methods as in [GL81], [GS85], and will be presented elsewhere.

4. Bifurcation varieties

Among the unfoldings of a codimension-3 singularity, one may expect to find an assortment of codimension-1 and codimension-2 singularities. This is indeed the case in the present problem. The existence and location of these lower codimension singularities is essential to the understanding of the original singularity. In this section, we locate and analyse varieties of dimension 2 and dimension 1, in the parameter space $\mathbb{R}^3$, corresponding to singularities (bifurcations) of codimension-1 and -2 respectively, in the systems (3.5), (2.17) and (2.10). All of these codimension-1 and -2 bifurcations have been studied previously and are now well understood. Therefore, we need only sketch their properties, and the proofs of their persistence. The first four cases were already seen in the previous section.

4.1. Primary bifurcation variety

The *primary bifurcation variety* $\mathscr{B}$ is the surface depicted in figure 4, generated by the parabolas in figure 1. Along a generic path transverse to $\mathscr{B}$, a solution with $\rho > 0$ bifurcates from the trivial solution $\rho = 0$. This must be thought of as a pitchfork bifurcation, even though, for the system (2.17), it appears to be what is often called a 'transcritical bifurcation' corresponding to the normal form $0 = \lambda x \pm x^2 = x(\lambda \pm x)$, which is not stable; see [GS85]. The explanation is that ρ, defined by $\rho = z_1\bar{z}_1 = r^2$, is an amplitude of an orbit with S^1 symmetry; elimination of the phase variable reduces a Hopf bifurcation in the original system to a pitchfork bifurcation in r (with $\mathbb{Z}_2$ symmetry from the half-period phase shift) and the substitution $\rho = r^2$ reduces this to the $\rho \geq 0$ half of a transcritical bifurcation with the trivial solution preserved. Thus we do have a codimension-1 pitchfork bifurcation on $\mathscr{B}$, and by the well known stability of the symmetric case, the bifurcation variety $\mathscr{B}$ is preserved for the full system, (except perhaps where additional degeneracies increase the codimension).

4.2. Limit point variety

The *limit point variety* $\mathscr{L}$ is the surface in parameter space generated by the ray $D = 0$ in figures 1 and 2, as β varies. On $\mathscr{L}$, a limit point or 'saddle-node bifurcation' occurs in (3.5), and this is well known to be a codimension-1 bifurcation. Therefore, $\mathscr{L}$ persists for $\epsilon \neq 0$ in (2.17), and when the phase equation (2.18) is restored, we obtain a saddle-node bifurcation of periodic orbits. This in turn persists as a two-dimensional variety for the original system, because the saddle-node bifurcation of periodic orbits also has codimension-1.

4.3. Symmetric cusp variety

The two surfaces $\mathscr{B}$ and $\mathscr{L}$ meet in the one-dimensional variety given by (3.13), which intersects the planes $\beta^2 = 1$ at the point $\mathscr{C}$ seen in figure 1. This corresponds to the familiar case of a degenerate pitchfork bifurcation with its cubic coefficient equal to 0, as in [GL81], [GS85]. It is the $\mathbb{Z}_2$ symmetric version of the standard cusp, and has codimension-2, with respect to symmetric perturbations. Here we will refer to it as the *symmetric cusp variety* $\mathscr{C}$. That the variety $\mathscr{C}$ persists for the full system follows from the preservation of S^1 symmetry on the periodic orbits, as in [GL81].

4.4. Double Hopf bifurcation variety

In the $\beta = 0$ plane, on the ray $\nu_2 = 0$, $\nu_1 < 0$, two Hopf bifurcations occur simultaneously in the original system, with the corresponding pure imaginary eigenvalues from (2.9) given by $\pm i(1 \pm |\mu_1|^{1/2})$. Since $|\mu_1|$ is small, this double Hopf bifurcation is determined by the classical non-resonant normal form, see [ILa80], [GH83]. This case has linear codimension-2, and occurs on the one-dimensional *double Hopf bifurcation variety* $\mathscr{B}^*$ in figure 2. As this situation is well known, we do not describe it further here, except to mention that typically it gives rise to mixed-mode secondary Hopf bifurcations (of 2-tori), and there is a possibility of a 3-torus arising from the interaction of these two Hopf bifurcations, as indicated in [ILa80] and proved in [Flo87].

4.5. Secondary Hopf bifurcation variety

Additional bifurcation varieties arising from (3.5) are revealed on investigation of the stability of the equilibria of (3.5) with $\rho > 0$, as determined by the eigenvalues of the Jacobian J_0 in (3.10). The eigenvalues σ of J_0 are roots of the characteristic polynomial

$$\sigma^3 + c_2\sigma^2 + c_1\sigma + c_0 = 0 \tag{4.1}$$

with coefficients given by

$$\begin{aligned} c_2 &= -\mathrm{tr}[J_0] = -4\beta \\ c_1 &= 4\beta^2 + 4v^2 - 2a\rho \\ c_0 &= \mp 4\rho\sqrt{D}. \end{aligned} \tag{4.2}$$

For local bifurcation to occur from a solution with $\rho > 0$, J_0 must have zero or imaginary eigenvalues. From (4.2) we see that J_0 cannot have a zero eigenvalue other than on $D = 0$; but this is the limit point variety $\mathscr{L}$ already considered. Necessary and sufficient conditions for J_0 to have non-zero imaginary eigenvalues are $c_1 > 0$ and

$$0 = c_0 - c_1c_2 = (4/b^2)(4(b^2+2)\beta^3 \pm 14a\sqrt{D}\beta^2 + 2(3D + abv_2)\beta \pm bv_2\sqrt{D}). \tag{4.3}$$

These conditions define a *secondary Hopf bifurcation variety* $\mathscr{H}$ in the parameter space. Note that the condition $c_1 > 0$ always holds when $a = -1$, but when $a = +1$, the magnitude of ρ becomes important. When these conditions hold, the pure imaginary eigenvalues associated with the secondary Hopf bifurcation are given by $\pm i\omega = \pm i\sqrt{c_1}$. It is rather difficult to solve (4.3) explicitly for (β, ν_1, μ_2). Instead, we consider asymptotic limits in which (4.3) is easy to solve analytically, and also we present numerical solutions in section 5.

Let us fix $\nu_1 < 0$, $a = \pm 1$, $b > 0$, and calculate an asymptotic approximation to $\nu_2(\beta)$ as $\beta \to 0$. We obtain, to first order

$$\begin{aligned} \nu_2 &= \mp 6\sqrt{-\nu_1}\,\beta + \mathcal{O}(\beta^2) \\ \rho &= \pm\frac{4}{b}\sqrt{-\nu_1}\,\beta + \mathcal{O}(\beta^2) \\ v &= \pm\sqrt{-\nu_1} - \frac{2a}{b}\beta + \mathcal{O}(\beta^2) \\ c_1 &= -4\nu_1 \mp 24\frac{a}{b}\sqrt{-\nu_1}\,\beta + \mathcal{O}(\beta^2). \end{aligned} \tag{4.4}$$

Note that $c_1 > 0$ for small $|\beta|$, regardless of the sign of a. The choice of upper or lower sign in the $\pm$ and $\mp$ terms is the same as that of the solution v in (3.7). We must choose the sign which yields $\rho > 0$ in (4.4). It then follows that

$$v_2 = -6\sqrt{-v_1}\,|\beta| + \mathcal{O}(\beta^2) < 0. \tag{4.5}$$

We conclude that for v_1 negative and bounded away from 0, the Hopf variety $\mathscr{H}$ is close to the lower branch of a parabola in the (v_1, v_2) plane, which lies between $\mathscr{B}$ and $\mathscr{L}$, asymptotically for $\beta \to 0$.

A similar analysis is possible for v_1 positive and bounded away from 0, except that here $\mathscr{H}$ can exist only in the case $a = -1$. The asymptotic approximations, as $\beta \to 0$, are

$$\begin{aligned} v_2 &= -bv_1 + \frac{b^2-3}{b}\beta^2 + \mathcal{O}(\beta^3) \\ v &= \frac{\beta}{b} + \mathcal{O}(\beta^2) \\ \rho &= v_1 + \frac{1-b^2}{b}\beta^2 + \mathcal{O}(\beta^3) \\ c_1 &= 2v_1 + \frac{3b^2+5}{b^2}\beta^2 + \mathcal{O}(\beta^2). \end{aligned} \tag{4.6}$$

Thus, for $v_1 > 0$, the Hopf variety $\mathscr{H}$ lies just below, and $\mathcal{O}(\beta^2)$ away from, the limit point variety $\mathscr{L}$, as $\beta \to 0$ in (v_1, v_2) coordinates.

The behaviour of $\mathscr{H}$ for v_1 near 0, and the question of whether the two branches for $a = -1$ are connected, are best left to the numerical investigations of the next section; see figures 5 and 6.

Finally, we remark that although our analysis has been for the truncated quadratic system (3.5), these Hopf bifurcations extend to the full three-dimensional system (3.4), provided the standard non-degeneracy conditions hold, see [GL81]. On restoring the phase equation (2.18), these periodic orbits trivially become 2-tori of the formal normal form (2.10). The scalings (3.3) ensure that this second frequency is very small compared to the original frequency $\omega = 1$ in (2.4). Therefore there can be no strong resonance. Normal hyperbolicity of the periodic orbit of (3.5), the generic case (and verified by numerical computation of the Floquet multipliers using AUTO), implies normal hyperbolicity of the 2-torus in (2.10). Together, these imply persistence of the 2-torus in the original system. The flow on the 2-torus will be either quasiperiodic, or so weakly resonant as to be practically indistinguishable from quasiperiodic. We conjecture that the flow on the torus will be quasiperiodic for a set in parameter space with measure tending to 1 as epsilon goes to 0, as in [SM84].

4.6. Bogdanov–Takens variety

Let us investigate the possibility of intersections of the Hopf bifurcation variety $\mathscr{H}$ and the limit point variety $\mathscr{L}$, each of codimension-1, as described above. This requires the conditions (4.3) and $D = 0$ to hold simultaneously, and then (4.3) reduces to

$$0 = c_0 - c_1 c_2 = \frac{8\beta}{b^2}(2(b^2+2)\beta^2 + abv_2). \tag{4.7}$$

This equation holds if $\beta = 0$, which we consider later, or if $\beta \neq 0$ and

$$\begin{aligned} \nu_1 &= -\left(1 + \frac{3}{b^2}\right)\beta^2 \\ \nu_2 &= -2\left(\frac{b^2+2}{ab}\right)\beta^2. \end{aligned} \tag{4.8}$$

Since $\nu_2 < 0$ on $\mathscr{H}$, the last equation restricts us to the case $a = +1$.

It is easy to verify that the characteristic polynomial (4.1) has a double zero root at the point (4.8), and that J_0 in (3.10) has rank 2, so the zero is non-semisimple. In fact, now $c_1 = 0$, so there are no longer any purely imaginary roots. The third eigenvalue of J_0 is clearly $\mathrm{tr} J_0 = 4\beta \neq 0$. Therefore we can transform J_0 to the Jordan form

$$J_{\mathrm{BT}} = \begin{pmatrix} 0 & 1 & 0 \\ 0 & 0 & 0 \\ 0 & 0 & 4\beta \end{pmatrix}. \tag{4.9}$$

In this situation, the well known Bogdanov–Takens bifurcation occurs, provided that the usual non-degeneracy conditions hold. (We have not verified them here, but it is the generic case). The equations (4.8) define a path in $\mathbb{R}^3$ which we call the *Bogdanov–Takens variety* $\mathscr{T}$. Note that for a given β, the Bogdanov-Takens variety (4.8) always lies to the left of the cusp variety (3.13), in the (ν_1, ν_2) plane. The intersection of $\mathscr{H}$ and $\mathscr{L}$, in a codimension-2 variety $\mathscr{T}$ with a double zero eigenvalue, has been observed also numerically; see section 5. The numerical computations also reveal homoclinic behaviour typically associated with Bogdanov–Takens bifurcations.

Assuming non-degeneracy of the Bogdanov–Takens bifurcation, it will certainly persist in the full three-dimensional system (2.17). However, in the four-dimensional normal form, we obtain a Bogdanov–Takens bifurcation of periodic orbits, which is much more complex than for equilibria. In particular, the homoclinic orbit can become a self-intersecting manifold, creating horseshoe chaos in the original system. This may be investigated further using Melnikov's method.

4.7. *The* $\{0, i, -i\}$ *variety*

Now consider the second possible solution of the equation (4.7), for simultaneous limit point and Hopf bifurcations, namely $\beta = 0$. When $\beta = 0$, it is clear that equation (4.3) holds only on the lines $\nu_2 = 0$ or $D = 0$. When $\nu_2 = 0$, the condition $D \geq 0$ implies that $\nu_1 \leq 0$. This is the codimension-2 double Hopf bifurcation variety $\mathscr{B}^*$ already discussed. On the line with $D = 0$ and $\beta = 0$, the condition $c_1 > 0$ for imaginary eigenvalues implies $a = -1$ and $\nu_1 > 0$. We conclude that zero and pure imaginary eigenvalues occur simultaneously along the ray $\{\beta = 0, D = 0, \nu_1 > 0\}$ of codimension-2, which we call the $\{0, \mathrm{i}, -\mathrm{i}\}$ *bifurcation variety* $\mathscr{L}^*$, shown in figure 2.

This codimension-2 bifurcation is studied in detail in section 6.

5. Numerical solutions using AUTO

Numerical computations of some representative bifurcation varieties and bifurcation diagrams have been carried out using AUTO, which is a general purpose software

package for the bifurcation analysis of differential equations, developed by E J Doedel [Doe86]. These computations confirm the analytical results of the previous section and complete the calculation of the secondary Hopf bifurcation variety $\mathscr{H}$. They also suggest some new phenomena, such as period doubling, which may have been missed in the normal form analysis. AUTO is capable of following paths of equilibrium or periodic solutions in a bifurcation parameter, determining stability in terms of eigenvalues or Floquet multipliers, detecting steady-state bifurcations, limit points, Hopf bifurcations, period doubling bifurcations, and torus bifurcations, and switching branches at bifurcation points. It can also follow paths of codimension-1 bifurcations in a two-parameter plane.

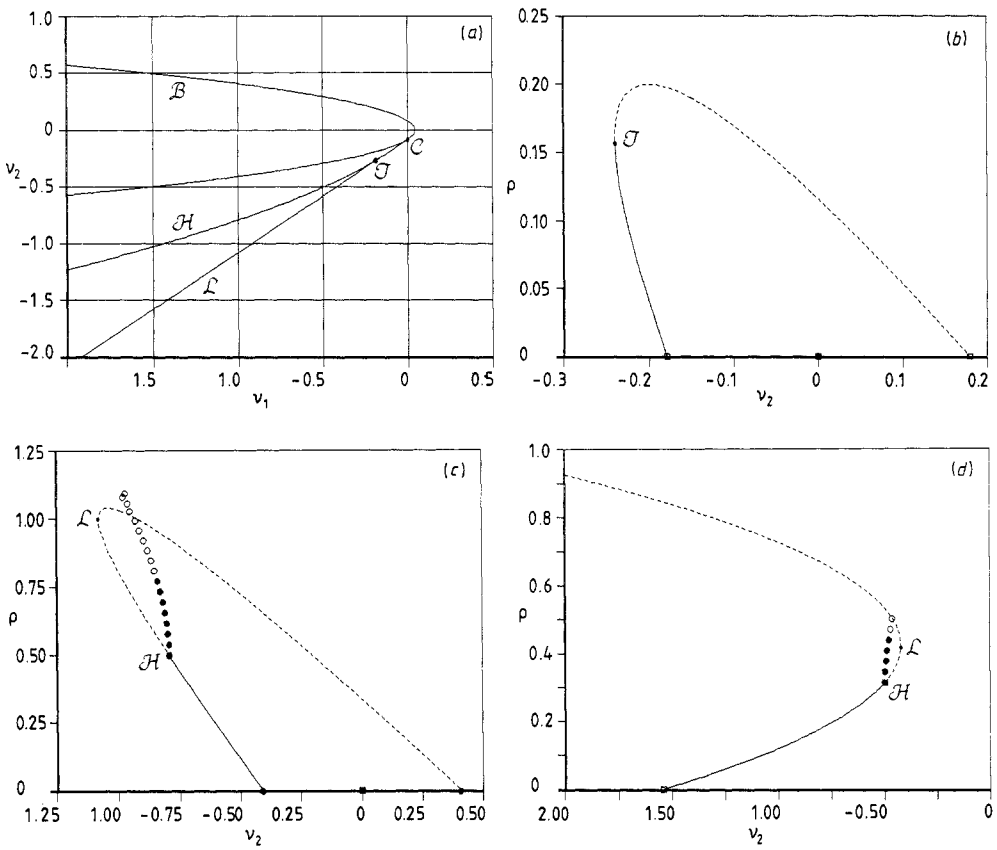

Figure 5. AUTO bifurcation diagrams for $a = +1$. See text for details.

Here we present a few representative diagrams from the application of AUTO to the system (3.5). In the bifurcation diagrams, full curves represent stable equilibrium solutions, broken curves represent unstable equilibrium solutions, full circles represent stable periodic solutions, and open circles represent unstable periodic solutions. Hopf bifurcation points are represented by full squares.

In figure 5, we have chosen $a = +1$, $b = +1$, and $\beta = -0.2$. The analysis in the previous section showed that, for $a = +1$, the limit point variety $\mathscr{L}$ and secondary Hopf variety $\mathscr{H}$ extend only to negative values of v_1 from a neighbourhood of the origin, and that they meet in a Bogdanov–Takens bifurcation $\mathscr{T}$. These features are

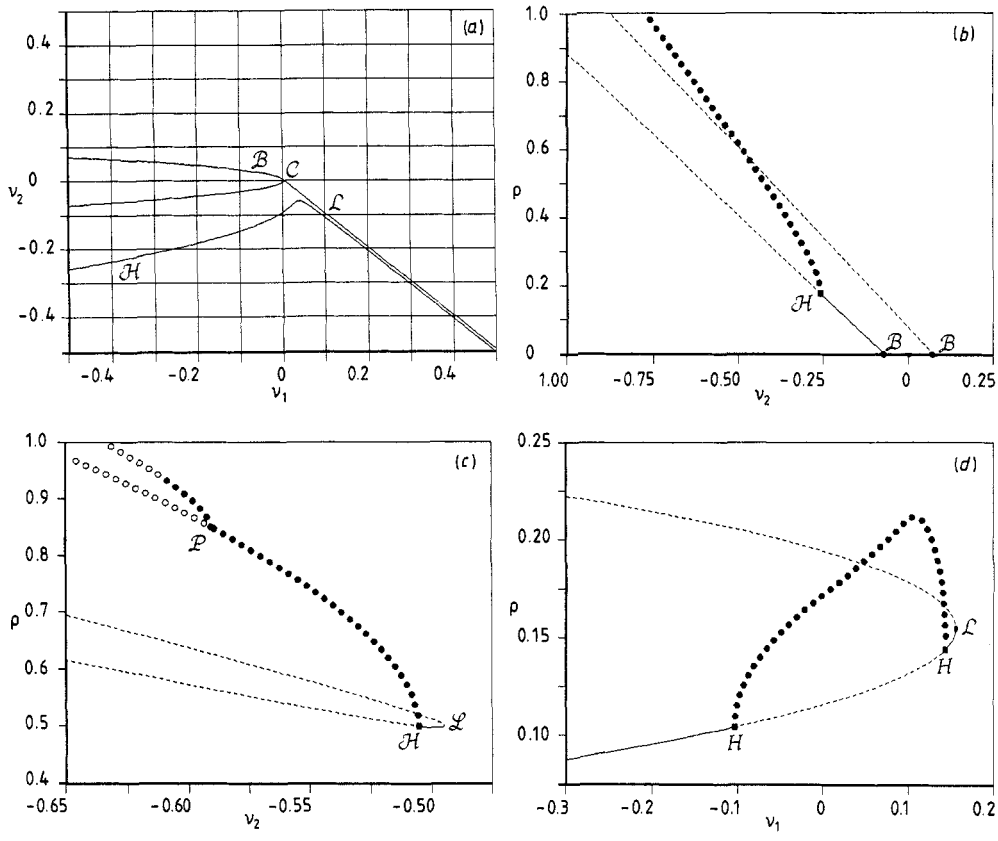

Figure 6. AUTO bifurcation diagrams for $a = -1$. See text for details.

confirmed numerically in these figures. Computations with other values of β, not shown here, gave qualitatively similar results, except that positive values of β yield different stabilities.

Figure 5(*a*) shows the codimension-1 bifurcation varieties $\mathscr{B}, \mathscr{L}, \mathscr{H}$, as curves in the (ν_1, ν_2) plane. The codimension-2 cusp variety $\mathscr{C}$, and Bogdanov–Takens variety $\mathscr{T}$, can be seen as the two points where the codimension-1 curves meet.

Figure 5(*b*) is a bifurcation diagram, with parameter ν_1 fixed, and ν_2 varying to pass through the Bogdanov–Takens point $(\nu_1, \nu_2) = (-0.16, -0.24)$ on $\mathscr{T}$. Numerical output from AUTO shows that two eigenvalues pass through 0 at this point, and change from real to complex at 0 as the parameter passes through $\mathscr{T}$.

Figure 5(*c*) shows a bifurcation diagram with parameter ν_2 varying and $\nu_1 = -1.0$ fixed, where all three codimension-1 varieties $\mathscr{B}$, $\mathscr{H}$, $\mathscr{L}$ exist, and it is clear that all three are crossed in this diagram. The loss of stability on the periodic branch is associated with a period-doubling bifurcation; AUTO detects a Floquet multiplier passing through -1 at this point. (It is possible to compute also the period doubled branch, but we have not done so in this diagram). The periodic branch ends with the period becoming 'infinite' (too large to continue computing) while the amplitude stays finite and close to the magnitude of the limit point. This is strong evidence of a homoclinic bifurcation, as can be expected, coming from the Bogdanov–Takens bifurcation.

Figure 5(*d*) is similar to 5(*c*), except that we have fixed $\nu_2 = -0.5031$, and let ν_1

be the bifurcation parameter. This gives a different view of the loss of stability of the periodic branch to a period-doubling bifurcation. Again the periodic branch ends with the period tending toward infinity, near the limit point of the equilibrium branch.

In figure 6, we have taken $a = -1$, $b = 1$, and $\beta = -0.05$. The asymptotic analysis of the previous section showed that when $a = -1$, the secondary Hopf variety $\mathscr{H}$ exists for both positive and negative values of ν_1, but we did not determine whether $\mathscr{H}$ is connected. Furthermore, we found that there is a $\{0, i, -i\}$ mode-interaction as $\beta \to 0$, when $\nu_1 > 0$.

Figure 6(*a*) shows the codimension-1 bifurcation varieties $\mathscr{B}, \mathscr{L}, \mathscr{H}$ as curves in the (ν_1, ν_2) plane, and the codimension-2 cusp variety $\mathscr{C}$, where $\mathscr{B}$ and $\mathscr{L}$ meet, as a point. The computations show that $\mathscr{H}$ is in fact connected and single-valued in ν_1, in an open neighbourhood of 0, and they confirm that $\mathscr{H}$ is very close to $\mathscr{L}$ for ν_1 sufficiently positive.

Figure 6(*b*) is a bifurcation diagram with parameter $\nu_1 = -0.5$ fixed, and ν_2 varying. It shows the two primary bifurcations $\mathscr{B}$, and the secondary Hopf bifurcation $\mathscr{H}$. Unlike the case $a = +1$ in figure 5, all three branches extend far from 0, without joining or terminating.

Figure 6(*c*) shows the bifurcation diagram with parameter $\nu_1 = +0.5$ fixed, and ν_2 varying. As in 6(*b*), it shows a secondary Hopf bifurcation $\mathscr{H}$, but the two primary bifurcations $\mathscr{B}$ have disappeared. Another difference from 6(*b*) is the appearance of a period-doubling bifurcation. Diagram 6(*c*) shows also the period-doubled branch, which in turn loses stability to a second period doubling.

Figure 6(*d*) is similar to 6(*c*), except with ν_1 chosen as bifurcation parameter, and with $\nu_2 = -0.15$ fixed. It shows the limit point $\mathscr{L}$, and *two* Hopf bifurcation points, joined by a 'loop' of periodic solutions. We should expect there to be two Hopf bifurcation points in this diagram because, as can be seen from figure 6(*a*), the line $\nu_2 = -0.15$ intersects the variety $\mathscr{H}$ in two points. Similar computations with values of ν_2 tending toward 0 show that these two Hopf bifurcations then coalesce and disappear, as one would expect from figure 6(*a*).

6. The $\{0, i, -i\}$-eigenvalue bifurcation

In this section we investigate a codimension-2 bifurcation, at which system (3.4) has a non-hyperbolic equilibrium with both zero and purely imaginary eigenvalues. After a time-rescaling, we may assume that these eigenvalues are $\{0, i, -i\}$. Such a bifurcation is well understood, see for instance [Lan79], [GH83], [CCH85], [Gil85]. The most important feature of this bifurcation is that in a generic two-parameter family a global Hopf bifurcation in $\mathbb{R}^2$ (corresponding to a 2-torus in $\mathbb{R}^3$) occurs in a reduced vector field, and the limit cycle is unique. Here we have *three* parameters. We will prove in this section that two of them unfold the singularity, i.e. with these two parameters the standard results apply. Moreover, we also show that the third parameter can be exploited to make the bifurcation degenerate. This degeneracy has, as far as we know, not been studied in general. Nevertheless, we can draw some interesting conclusions. In this three parameter space there is a line where a degenerate Hopf bifurcation occurs, i.e. the first focal value, or stability coefficient, vanishes. This line is the boundary of a codimension-1 submanifold of saddle-node bifurcations of periodic orbits in the parameter space. We conjecture that these saddle-node bifurcations are non-degenerate and that consequently at most two periodic orbits can occur. The non-degeneracy of

the saddle-node bifurcation in this three parameter family has not yet been shown in general.

It turns out, as we will show below, that for restricted values of the parameters the system (3.4) is *time-reversible*, up to the lowest order in ϵ, and hence is not in the generic class of systems discussed in [GH83], [CCH85], [Gil85], [Zol84]. This complicates the analysis substantially. We have used MAPLE to do the so-called 'straightforward but lengthy computations'.

Recall system (3.4)

$$\begin{aligned}\dot{\rho} &= 2\rho(\beta + u + \epsilon d_1\rho + \mathcal{O}(\epsilon^2))\\ \dot{u} &= v_1 - u^2 + v^2 + a\rho + \epsilon d_3\rho v + \mathcal{O}(\epsilon^2)\\ \dot{v} &= v_2 - 2uv + b\rho + \epsilon d_4\rho v + \mathcal{O}(\epsilon^2).\end{aligned} \tag{6.1}$$

Recall from subsection 4.7 that the $\{0, \mathrm{i}, -\mathrm{i}\}$ bifurcation occurs only if $a = -1$ and $v_1 > 0$, which we assume throughout this section. Let us fix $v_1 = 1$, thereby defining the scaling of ϵ in (3.3). Our parameters are now $\{\epsilon, \beta, v_2\}$. The rescaling (3.3) implies that any real values (not necessarily small) of β and v_2 will be relevant to the original system. Recall that when $\epsilon = 0$ the derivative of the right hand side of (6.1) at the non-trivial equilibrium is

$$J_0 = \begin{pmatrix} 0 & 2\rho & 0 \\ a & 2\beta & 2v \\ b & -2v & 2\beta \end{pmatrix} \tag{6.2}$$

with the determinant given by (3.8) and (3.11). The $\{0, \mathrm{i}, -\mathrm{i}\}$ bifurcation occurs on the ray $\mathscr{L}^* = \{\beta = 0,\ D = 0,\ v_1 > 0\}$, shown in figure 2. If $v_1 = 1$, then the $\{0, \mathrm{i}, -\mathrm{i}\}$-point occurs for $(\beta, v_1, v_2) = (0, 1, -b)$ (recall that $D = \beta = 0$ implies that $v_2 = (b/a)\, v_1$) and the relevant equilibrium is $(\rho, u, v) = (1, 0, 0)$. We replace $\rho \equiv 1 + \tilde{\rho}$ and $v_2 \equiv -b + v_3$. Now consider (ϵ, β, v_3) as small parameters. With these choices, the origin in parameter space is a $\{0, \mathrm{i}, -\mathrm{i}\}$ bifurcation point, and the origin in state space is the non-hyperbolic equilibrium. Here the matrix J_0 becomes

$$A = \begin{pmatrix} 0 & 2 & 0 \\ -1 & 0 & 0 \\ b & 0 & 0 \end{pmatrix}. \tag{6.3}$$

The matrix A has eigenvalues $\{0, \pm\mathrm{i}\sqrt{2}\}$ for all values of b.

We first concentrate on the linear part of the vector field. We apply the linear transformation with the matrix

$$\begin{pmatrix} 1 & 0 & 0 \\ 0 & 1 & 0 \\ 0 & -b & b \end{pmatrix}. \tag{6.4}$$

We rescale u by $1/\sqrt{2}$ and we set

$$\begin{aligned}\mu_1 &= \epsilon\\ \mu_2 &= \sqrt{2}\beta\\ \mu_3 &= \frac{\sqrt{2}v_3}{2b}.\end{aligned} \tag{6.5}$$

This gives the following system of equations:

$$\begin{aligned}
\dot{\rho} &= u + \rho u + \mu_1(d_1\sqrt{2} + 2d_1\sqrt{2}\,\rho + d_1\sqrt{2}\,\rho^2) + \mu_2(1+\rho) + \mathcal{O}(\mu_1^2)\\
\dot{u} &= \frac{b^2u^2}{2} + b^2v^2 - \frac{u^2}{2} - \rho - b^2uv\sqrt{2} + \mu_1\left(d_3bv + d_3b\rho v - \frac{bd_3u\sqrt{2}}{2} - \frac{bd_3\rho u\sqrt{2}}{2}\right)\\
&\quad + \mathcal{O}(\mu_1^2) \qquad (6.6)\\
\dot{v} &= -b^2uv - uv + \frac{b^2v^2\sqrt{2}}{2} + \frac{b^2u^2\sqrt{2}}{4} + \frac{u^2\sqrt{2}}{4} + \frac{\mu_1}{2}(-d_3\rho bu - d_4u - d_4\rho u\\
&\quad + bd_3v\sqrt{2} + bd_3\rho v\sqrt{2} + d_4v\sqrt{2} + d_4\rho v\sqrt{2} - d_3bu) + \mu_3 + \mathcal{O}(\mu_1^2).
\end{aligned}$$

From this equation it is evident that the unperturbed equation, i.e. $\mu_i = 0$, is time-reversible. The symmetry is given by

$$u \to -u \qquad s \to -s \qquad x \to x \qquad t \to -t. \tag{6.7}$$

If we put this unperturbed vector field into Birkhoff normal form, with $z = x - iu$ and $y = v$

$$\begin{aligned}
\dot{z} &= z\,f(|z|^2, y) + \mathcal{O}(|z| + |y|)^N\\
\dot{y} &= g(|z|^2, y) + \mathcal{O}(|z| + |y|)^N
\end{aligned} \tag{6.8}$$

where f (complex) and g (real) vanish at the origin, then time-reversibility implies that, as functions of y, g is even, the even part of f is purely imaginary and the odd part of f is real. This symmetry complicates the computations substantially. We would like to apply the standard results on the unfolding of the linear vector field with eigenvalues $\{0, i, -i\}$, see [GH83], [CCH85], [Gil85], [Zol84]. To do so we need to consider an equation in the plane of $|z| = q$ and y. Due to the above time-reversal symmetry, cubic coefficients in the equations in q and y that would have to satisfy a certain non-degeneracy condition, instead vanish *identically*. The system is degenerate, in fact to any order. It would not help to include higher-order terms. We therefore conclude that it is necessary to compute the dependence of (6.8) on the small parameters.

We cannot simply follow the singularity in the small parameters (μ_1, μ_2, μ_3), because of the presence of a zero eigenvalue. Instead we rename the x_3 component of the equilibrium, say $x_3 = \alpha$ and choose parameters (μ_1, μ_2, α). Now μ_3 and x_1, x_2 depend on (μ_1, μ_2, α). Instead of α we will write μ_3 again, thus changing the meaning of this parameter.

Next, we introduce complex coordinates

$$z = qe^{i\theta} = \rho - iu \qquad y = v$$

and put the linear part with respect to the parameters in Jordan normal form. The linear part of the vector field becomes

$$\begin{pmatrix} i + p_1 & 0 & 0\\ 0 & -i + \bar{p}_1 & 0\\ 0 & 0 & p_2 \end{pmatrix} \tag{6.9}$$

where

$$\begin{aligned} p_1 &= \mu_1(-\tfrac{1}{4}\sqrt{2}bd_3 - \tfrac{1}{2}\sqrt{2}b^2d_1 + \sqrt{2}d_1) + \mu_2(\tfrac{1}{2} - \tfrac{1}{2}b^2) - \tfrac{1}{2}b^2\sqrt{2}\mu_3 + \mathcal{O}(|\mu|^2) \\ p_2 &= \mu_1(\sqrt{2}d_1 + \tfrac{1}{2}\sqrt{2}d_4 + \sqrt{2}b^2d_1 + \tfrac{1}{2}b\sqrt{2}d_3)\mu_2(b^2+1) + \sqrt{2}b^2\mu_3 + \mathcal{O}(|\mu|^2). \end{aligned} \tag{6.10}$$

It is remarkable that p_1 is real up to second order in μ. Next we use near-identity transformations to put the nonlinear vector field into normal form. To arbitrarily high order we can divide out an additional S^1 symmetry. Thus, to this order we reduce to a two-dimensional equation in q and y, which has the following form:

$$\begin{aligned} \dot{q} &= \tau(\mu)q - B(\mu)qy + c_1(\mu)q^3 + c_2(\mu)qy^2 + d_1(\mu)qy^3 + d_2(\mu)q^3y \\ &\quad + \mathcal{O}((|q| + |y|)^5 + |\mu|^5) \\ \dot{y} &= 2\delta(\mu)q + q^2 + y^2 + c_3(\mu)q^2y + c_4(\mu)y^3 + d_3(\mu)q^2y^2 + d_4(\mu)y^4 \\ &\quad + \mathcal{O}((|q| + |y|)^5 + |\mu|^5). \end{aligned} \tag{6.11}$$

It turns out that

$$B(\mu) = 1 + \mathcal{O}(\mu^2). \tag{6.12}$$

We introduce the following notation:

$$\begin{aligned} \tau(\mu) &= \langle \tau_1, \mu \rangle + \mathcal{O}(\mu^2) \\ \delta(\mu) &= \langle \delta_1, \mu \rangle + \mathcal{O}(\mu^2) \\ c_i(\mu) &= \langle c_{i1}, \mu \rangle + \mathcal{O}(\mu^2) \\ d_i(\mu) &= d_{i0} + \mathcal{O}(\mu). \end{aligned} \tag{6.13}$$

We perform the transformation $y = \tilde{y} + r(\mu)$ and choose $r(\mu)$ such that the linear term in y in the second equation vanishes

$$r(\mu) = -\langle \delta_1, \mu \rangle + \mathcal{O}(\mu^2).$$

A rescaling of y and q of the form $y = (1 + \mathcal{O}(\mu^2))\tilde{y}$ and $q = (1 + \mathcal{O}(\mu^2))\tilde{q}$ can be chosen such that the coefficients of y^2 and q^2 in the second equation of (6.11) become 1 again. System (6.11) is transformed to

$$\begin{aligned} \dot{q} &= \kappa(\mu)q - \tilde{B}(\mu)qy + \tilde{c}_1(\mu)q^3 + \tilde{c}_2(\mu)qy^2 + \tilde{d}_1(\mu)qy^3 + \tilde{d}_2(\mu)q^3y \\ &\quad + \mathcal{O}((|q| + |y|)^5 + |\mu|^5) \\ \dot{y} &= -\tilde{\delta}(\mu)^2 + q^2 + y^2 + \tilde{c}_3(\mu)q^2y + \tilde{c}_4(\mu)y^3 + \tilde{d}_3(\mu)q^2y^2 + \tilde{d}_4(\mu)y^4 \\ &\quad + \mathcal{O}((|q| + |y|)^5 + |\mu|^5) \end{aligned} \tag{6.14}$$

where

$$\begin{aligned} \kappa(\mu) &= \langle (\tau_1 + \delta_1), \mu \rangle + \mathcal{O}(\mu^2) = \langle \kappa_1, \mu \rangle + \mathcal{O}(\mu^2) \\ \tilde{B}(\mu) &= 1 + \mathcal{O}(\mu^2) \\ \tilde{c}_i(\mu) &= c_i(\mu) + \mathcal{O}(\mu^2) \\ \tilde{d}_i(\mu) &= d_i(\mu) + \mathcal{O}(\mu^2) \\ \tilde{\delta}(\mu) &= \langle \delta_1, \mu \rangle + \mathcal{O}(\mu^2). \end{aligned} \tag{6.15}$$

It turns out that

$$\left.\frac{\partial(\kappa,\tilde{\delta})}{\partial(\mu_1,\mu_2)}\right|_{\mu_1=\mu_2=\mu_3=0}=\frac{\sqrt{2}\ (2b^2d_1+b^2d_4-2bd_3+2d_1-d_4)}{4}. \tag{6.16}$$

Provided that this expression is non-zero we can take as our new parameters $(\kappa,\tilde{\delta},\mu_3)$. We drop the $\tilde{}$ and apply the rescalings

$$q=\delta\tilde{q}\qquad y=\delta\tilde{y}\qquad \kappa=\delta^3\tilde{\kappa}\qquad \mu_3=\delta\tilde{\mu}_3\qquad \delta t=\tilde{t}. \tag{6.17}$$

Dropping the $\tilde{}$ and writing

$$\langle c_{i1},\mu\rangle=C_{i1}\delta+C_{i2}\kappa+C_{i3}\mu_3 \tag{6.18}$$

gives the system of equations

$$\begin{aligned}\dot{q}&=(-1+\mathcal{O}(\delta^2))qy+\delta^2(\kappa q+(C_{11}+C_{13}\mu_3)q^3+(C_{21}+C_{23}\mu_3)qy^2\\&\qquad+d_1(0)qy^3+d_2(0)q^3y)+\mathcal{O}(\delta^3)\\\dot{y}&=-1+q^2+y^2+\delta^2((C_{31}+C_{33}\mu_3)q^2y+(C_{41}+C_{43}\mu_3)y^3\\&\qquad+d_3(0)q^2y^2+d_4(0)y^4)+\mathcal{O}(\delta^3).\end{aligned} \tag{6.19}$$

We repeat some of the standard facts about this specific codimension-2 problem that we need here (see [GH83], [Zol84], [CCH85], [Gil85]). Consider the truncation at order two. If $\kappa=0$ then the system

$$\begin{aligned}\dot{q}&=-qy\\\dot{y}&=-1+q^2+y^2\end{aligned} \tag{6.20}$$

is integrable with integral

$$H(q,y)=\frac{-q^2}{2}\left(-1+y^2+\frac{q^2}{2}\right). \tag{6.21}$$

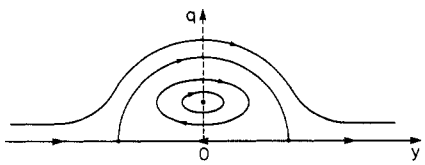

Figure 7. Level sets of H.

The condition for (6.19) to have a periodic solution close to the compact level set γ_h of (6.21) (see figure 7) becomes

$$\mathscr{G}(h, \delta) = 0$$

where

$$\mathscr{G} = \tilde{\tau} \oint_{\gamma_h} q \, dy + (C_{11} + C_{13}\mu_3) \oint_{\gamma_h} q^3 \, dy + (C_{21} + C_{23}\mu_3) \oint_{\gamma_h} q y^2 \, dy$$
$$- (C_{31} + C_{33}\mu_3) \oint_{\gamma_h} q^2 y \, dq - (C_{41} + C_{43}) \oint_{\gamma_h} y^3 \, dq + \mathscr{O}(\delta).$$

If we let

$$I_j = I_j(h) = \oint_{\gamma_h} q^{j+1} y \, dq \tag{6.22}$$

then integration by parts simplifies this expression to

$$\mathscr{G}(h, \delta) = I_0\left(K_1 + K_2 \frac{I_2}{I_0}\right) + \mathscr{O}(\delta) \tag{6.23}$$

where

$$\begin{aligned} K_1 &= \kappa - 3(C_{41} + C_{43}\mu_3) - 2(C_{21} + C_{23}\mu_3) \\ K_2 &= -(C_{31} + C_{33}\mu_3) - 4(C_{11} + C_{13}\mu_3) + 3(C_{41} + C_{43}\mu_3) + 2(C_{21} + C_{23}\mu_3). \end{aligned} \tag{6.24}$$

As we expect, the formulae for K_1 and K_2 are complicated; however, if $K_2 \neq 0$ then the bifurcation is non-degenerate. So the most interesting fact is that K_2 depends in a generic way on the third parameter μ_3.

Theorem 2. Assume that $6d_1 + d_4 \neq 0$ and $2b^2d_1 + b^2d_4 - 2bd_3 + 2d_1 - d_4 \neq 0$. Then $dK_2/d\mu_3 \neq 0$.

Proof. This fact follows from the identity

$$K_2 = \mu_3\left(\frac{16(6d_1 + d_4)}{(b^2+1)\sqrt{2}\,(2b^2d_1 + b^2d_4 - 2bd_3 + 2d_1 - d_4)}\right)$$
$$+ \frac{1}{(18b^2+18)(2b^2d_1 + b^2d_4 - 2bd_3 + 2d_1 - d_4)b^2}$$
$$\times -(740b^4d_1 + 50b^6d_1 - 50b^5d_3 + 1122b^2d_1 - 273b^2d_4$$
$$-690b^3d_3 + 320b^4d_4 + 25b^6d_4 + 1296d_1 + 216d_4).$$

Corollary 1. If $K_1/K_2 = -Q(h) \equiv I_2(h)/I_0(h)$, then (6.19) has a unique periodic orbit close to γ_h. The level set $K_1/K_2 = -1$ is the locus in parameter space of Hopf bifurcation. The level set $K_1/K_2 = -4/5$ is the locus of saddle connections. This follows from (6.23), evaluating the integrals at the centre and the saddle connection.

Corollary 2. There is the possibility of a degenerate Hopf bifurcation. If we set $K_2 = 0$, then we determine a codimension-1 submanifold on which the fifth-order terms in the normal form equation will determine the bifurcation. For instance, for the points of Hopf bifurcation this corresponds to points in parameter space where the first stability coefficient is zero. This will (in the simplest possible scenario) lead to a codimension-1 submanifold of saddle-node bifurcations of periodic orbits in the parameter space. This follows from the fact that in this degenerate case we must solve an equation of the type

$$\mathcal{G}(h, v, \delta) = I_0\left(L_0 + vh + L_1\frac{I_2}{I_0}\right) + \mathcal{O}(\delta) = 0.$$

For nearby parameter values there will be multiple periodic orbits, see figure 8. To locate these one would have to calculate the fifth-order terms, which we have not yet done.

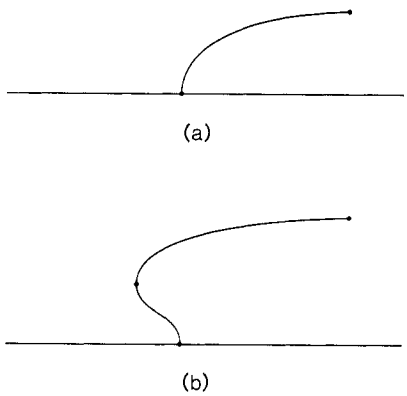

Figure 8. Degenerate Hopf bifurcation.

The analysis of this section captures the existence of phenomena of at least the same complexity as found in previous studies of the non-resonant double Hopf bifurcation. Moreover, it shows the existence of neutrally stable periodic orbits in (6.19), although we have not yet located where this happens in parameter space and what the order of degeneracy will be. From the work of [CSG87], [Zol87] we know that generically this does not happen in the non-resonant case. In the region of normal hyperbolicity the existence of a periodic solution to (6.19) implies the existence of a *normally hyperbolic three frequency solution* to (6.1) even if the S^1 symmetry in this equation is broken (at sufficiently high order).

We would like to know what happens at the points where (in the original system) a 2-torus bifurcates to a 3-torus. This has been investigated, for the general case, in [ILo88]. However, there are two additional complications here. The three frequencies are of different orders of magnitude, due to the two essential rescalings we have made in (3.3),(6.17). Also, the occurrence of the degeneracy suggests that there will be a saddle-node bifurcation of 3-tori. Chenciner [Che83] studied a degenerate Hopf bifurcation for maps of $\mathbb{R}^2$; that is, for 2-tori. His results imply that a three-dimensional system such as (3.4) could have the following dynamics.

- For values of parameters in a Cantor set tangent to the hyperplane of Hopf bifurcation there would exist a neutrally stable 2-torus.
- Each point in the Cantor set would be the centre of a two-sided cone such that for parameter values in the interior of the cone, there would exist a normally hyperbolic 2-torus. In one component of the cone, the tori would be stable and in the other they would be unstable.
- At a point of intersection of the two cones, there would exist multiple 2-tori. The regions of stability of the 2-tori would be very small and other kinds of complex dynamics would occur. In particular the system would have an infinite number of periodic orbits with arbitrarily long period, transversal homoclinic orbits and orbits with homoclinic tangency.

It has yet to be verified that the results on degenerate bifurcations of tori, such as in [Che83], [BBH90], [ILo88], do apply to our original four-dimensional system.

Acknowledgments

The authors would like to thank Henk Broer, Richard Cushman, Gérard Iooss, Jan Cees van der Meer, Jan Sanders and André Vanderbauwhede for helpful discussions, and also to thank a referee for suggesting improvements in the treatment of the normal form. This work was supported in part by the Natural Sciences and Engineering Research Council of Canada, and by the Institute for Mathematics and its Applications, Minnesota, USA.

References

[AC80] Ashkenazi M and Chow S N 1980 A Hopf's bifurcation theorem for nonsimple eigenvalues *Adv. Appl. Math.* **1** 360–72

[AH85] Atadan A S and Huseyin K 1985 Analysis of dynamical bifurcations in the case of nonsimple eigenvalues *IEEE Proc. Int. Symp. on Circuits and Systems* vol 2 pp 871–2

[Arn71] Arnold V I 1971 On matrices depending on parameters *Russ. Math. Surveys* **26** 29–43

[BBH90] Braaksma B L J, Broer H W, and Huitema G B 1990 Towards a quasi periodic bifurcation theory *Mem. AMS* **83** 83–175

[Bro81] Broer H W 1981 Formal normal form theorems for vector fields and some consequences for bifurcations in the volume preserving case *Dynamical Systems and Turbulence, Warwick 1980* ed D A Rand and L-S Young *Lecture Notes in Math.* **898** pp 54–74 (Berlin: Springer)

[Bru89] Bruno A D 1989 *Local Methods in Nonlinear Differential Equations* (Berlin: Springer)

[CCH85] Carr J, Chow S N, and Hale J K 1985 Abelian integrals and bifurcation theory *J. Diff. Eq.* **59** 413–36

[Che83] Chenciner A 1983 Bifurcations de difféomorphismes de 122^2 au voisinage d'un point fixe elliptique *Chaotic Behaviour of Deterministic Systems* ed R G H Helleman, G Iooss and R Stora (Amsterdam: North-Holland) pp 273–348

[CMN84] Caprino S, Maffei C, and Negrini P 1984 Hopf bifurcation at 1:1 resonance *Nonlin. Anal. Theor. Meth. Appl.* **8** 1011–32

[CS86] Cushman R and Sanders J A 1986 Nilpotent normal forms and representation theory of sl(2,$\mathbb{R}$) *Multiparameter Bifurcation Theory* ed M Golubitsky and J Guckenheimer *Contemp. Math.* **56** 31–51 (Providence, RI: American Mathematical Society)

[CSG87] Carr J, Sanders J A, and van Gils S A 1987 Nonresonant bifurcations with symmetry *SIAM J. Math. Anal.* **18** 579–91

[Cus82] Cushman R 1982 Reduction of the 1:1 non-semisimple resonance *Hadron. J.* **5** 2109–24

[Doe86] Doedel E J and Kernevez J-P 1986 AUTO: Software for continuation and bifurcation problems in ordinary differential equations *Appl. Math. Rep.* (Pasadena, CA: California Institute of Technology)

[ETB87] Elphick C, Tirapegui E, Brachet M E, Coullet P, and Iooss G 1987 A simple global characterization for normal forms of singular vector fields *Physica* **29D** 95–127

[Flo87] Flockerzi D 1987 Persistence and bifurcation of invariant tori *Oscillation, Bifurcation and Chaos* ed F V Atkinson, W F Langford and A B Mingarelli *CMS Conf. Proc.* vol 8 pp 419–41

[GH83] Guckenheimer J and Holmes P 1983 *Nonlinear oscillations, dynamical systems and bifurcations of vector fields* (*Appl. Math. Sci.* **42**) (Berlin: Springer)

[GIL] van Gils S A, Iooss G, and Los J E 1990 On the persistence of 3-tori in the 1:1 resonance. In preparation

[Gil85] van Gils S A 1985 A note on: Abelian integrals and bifurcation theory *J. Diff. Eq.* **59** 437–41

[GL81] Golubitsky M and Langford W F 1981 Classification and unfoldings of degenerate Hopf bifurcations *J. Diff. Eq.* **41** 375–415

[GS85] Golubitsky M and Schaeffer D G 1985 *Singularities and Groups in Bifurcation Theory* vol 1 (Berlin: Springer)

[GSS88] Golubitsky M, I Stewart, and Schaeffer D G 1988 *Singularities and Groups in Bifurcation Theory* vol 2 (Berlin: Springer)

[ILa80] Iooss G and Langford W F 1980 Conjectures on the routes to turbulence via bifurcations *Nonlinear Dynamics* ed R H G Helleman *Ann. NY Acad. Sci.* **357** 489–505

[ILo89] Iooss G and Los J E 1989 Quasi-codimension 3 bifurcation of invariant T^2 tori for maps *Proc. Int. Conf. on Bifurcation Theory and its Numerical Analysis* (Xi'an, China: Xian Jiaotong University Press) pp 36–50

[ILo88] Iooss G and Los J E 1988 Quasi-genericity of bifurcations to high dimensional invariant tori for maps *Commun. Math. Phys.* **119** 453–500

[KH74] Kopell N and Howard L N 1974 Bifurcations under nongeneric conditions *Adv. Math.* **13** 274–83

[Kru86] Krupa M 1986 On 1:1 Resonant Hopf Bifurcation *MSc* Department of Pure Mathematics, University of Waterloo, Canada

[Kru90] Krupa M 1990 Bifurcations of relative equilibria *SIAM J. Math. Anal.* to appear

[Lan79] Langford W F 1979 Periodic and steady-state mode interactions lead to tori *SIAM J. Appl. Math.* **37** 22–48

[Mee85] van der Meer J 1985 *The Hamiltonian Hopf Bifurcation. Lecture Notes in Math.* **1160** (Berlin: Springer)

[MM76] Marsden J E and McCracken M 1976 *The Hopf Bifurcation and its Applications. Appl. Math. Sci.* vol 19 (Berlin: Springer)

[Mey84] Meyer K R 1984 Normal forms for the general equilibrium *Funkcialaj Ekvacioj* **27** 261–71

[MS71] Meyer K R and Schmidt M S 1971 Periodic orbits near $l4$ for mass ratios near the critical mass ratio of Routh *Celest. Mech.* **4** 99–109

[SM84] Scheurle J and Marsden J 1984 Bifurcation to quasi-periodic tori in the interaction of steady state and Hopf bifurcations *SIAM J. Math. Anal.* **15** 1055–74

[Van86] Vanderbauwhede A 1986 Hopf bifurcation at non-semisimple eigenvalues *Multiparameter Bifurcation Theory* ed M Golubitsky and J Guckenheimer *Contemp. Math.* **56** 343–53 (Providence, RI: American Mathematical Society)

[Zol84] Zoladek H 1984 On the versality of a family of symmetric vector fields in the plane *Math. USSR Sb.* **48** 463–92

[Zol87] Zoladek H 1987 Bifurcations of certain families of planar vector fields tangent to the axes *J. Diff. Eq.* **67** 1–55